0026-895X/99/030720-08$3.00/0

MOLECULAR PHARMACOLOGY, **56:**720–727 (1999).

Properties of the Novel ATP-Gated Ionotropic Receptor Composed of the $P2X_1$ and $P2X_5$ Isoforms

WILLIAM R. HAINES, GONZALO E. TORRES, MARK M. VOIGT, and TERRANCE M. EGAN

Department of Pharmacological and Physiological Sciences, St. Louis University School of Medicine, St. Louis, Missouri

Received April 21, 1999; accepted July 2, 1999

This paper is available online at http://www.molpharm.org

ABSTRACT

We recently reported that a novel hetero-oligomeric P2X receptor is formed from the $P2X_1$ and $P2X_5$ isoforms when coexpressed in human embryonic kidney 293 cells (Torres et al., 1998). A more complete description of the pharmacology of this novel receptor is presented here. A brief application of ATP to a voltage-clamped cell transiently expressing $P2X_{1/5}$ receptors resulted in a biphasic current that rapidly reached a peak and then decayed to a sustained plateau. Washout of ATP was accompanied by generation and fade of a pronounced tail of inward current. EC_{50} values were determined from concentration-response curves for a range of agonists. The rank order of agonist potency was ATP $\geq$ 2 methylthio ATP $>$ adenosine 5′-*O*-(3-thiotriphosphate) $>$ α,β-methylene ATP $>$ ADP $>$ CTP. α,β-methylene ADP, UTP, GTP, and AMP were ineffective. Only ATP and 2 methylthio ATP were full agonists. IC_{50} values were determined from concentration-response curves for three commonly used purinergic antagonists. Suramin and pyridoxal phosphate-6-azophenyl-2′, 4′-disulfonic acid were equipotent at $P2X_1$ and $P2X_{1/5}$ receptors; however, the $P2X_{1/5}$ receptor was much less sensitive to TNP-ATP than was the $P2X_1$ receptor. The amplitude of peak ATP-gated current was relatively insensitive to changes in $[Ca^{2+}]_O$ (1–30 mM). Finally, plateau currents were potentiated by low concentrations of pyridoxal phosphate-6-azophenyl-2′, 4′-disulfonic acid and by raising $[Ca^{2+}]_O$. These results provide additional information on the pharmacological profile of the recombinant $P2X_{1/5}$ receptor channel and provide a basis to further evaluate ATP-induced currents in native tissues.

Extracellular ATP-mediated signaling is achieved in part through activation of a family of P2X receptors that conduct the flow of sodium, potassium, and calcium across cell-surface membranes (Bean and Friel, 1993; Surprenant et al., 1995; Brake and Julius, 1996). Activation of these ionotropic receptors produces a sudden change in membrane potential that initiates a variety of physiological functions including smooth muscle contraction, neuroendocrine secretion, synaptic transmission, and the perception of pain (Ralevic and Burnstock, 1998).

To date, seven different P2X isoforms have been discovered through cDNA cloning. With the single exception of the $P2X_6$ isoform, each can form a functional homo-oligomeric receptor with a distinct pharmacological and biophysical profile when individually expressed in heterologous cell systems (Torres et al., 1999). In many cases, the phenotypes of native ATP-gated currents match those of the recombinant homomeric P2X receptor. For example, currents recorded from oocytes expressing the $P2X_1$ receptor closely resemble the native ATP-mediated response of the rat vas deferens (Valera et al., 1994; Khakh et al., 1995; Collo et al., 1996). However, it is often difficult to equate a native response with current through a recombinant homo-oligomeric receptor. This may be because additional P2X isoforms exist that have yet to be cloned, the native response is modulated by a regulatory pathway that is missing in the heterologous systems, or some native receptors are hetero-oligomeric complexes of different P2X isoforms. The formation of functional ion channels by heteromeric assembly of different isoforms is not without precedent; heteromultimeric nicotinic, glutamatergic, and glycinergic receptors are examples (Betz, 1990; Barnard, 1992; Claudio, 1992). The hypothesis that P2X receptors also can form hetero-oligomeric assemblies is supported by data that show that individual isoforms coimmunoprecipitate in a number of different but specific heteromeric combinations (Torres et al., 1999). Furthermore, many tissues contain mRNA for multiple P2X receptor isoforms (Collo et al., 1996; Vulchanova et al., 1997). One example is the overlap of mRNA expression of the $P2X_1$ and $P2X_5$ isoforms in the ventral horn of the spinal cord (Collo et al., 1996). We have recently demonstrated that a novel $P2X_{1/5}$ receptor can form from the coexpression of $P2X_1$ and $P2X_5$ in human embryonic

This work was supported by National Institutes of Health Grants HL56236 (T.M.E.) and NS35534 (M.M.V.) and an American Heart Association Missouri Affiliate Predoctoral Fellowship 9804090X (W.R.H).

ABBREVIATIONS: PPADS, pyridoxal phosphate-6-azophenyl-2′,4′-disulfonic acid; α,β-meADP, α,β-methylene ADP; α,β-meATP, α,β-methylene ATP; ATPγS, adenosine 5′-*O*-(3-thiotriphosphate); TNP-ATP, 2′,3′-*O*-(2,4,6-trinitrophenyl) ATP; 2-meSATP, 2-methylthio ATP; HEK, human embryonic kidney.

kidney (HEK)-293 cells (Torres et al., 1998). Here we provide a more complete description of the pharmacology and biophysics of this novel $P2X_{1/5}$ receptor channel. The data will be helpful in determining the subunit composition of native receptors of excitable tissues.

Materials and Methods

DNA Constructs. The wild-type $P2X_1$ receptor cDNA was cloned from a rat heart cDNA library provided by Dr. M. Tamkun (Vanderbilt University, Nashville, TN). $P2X_5$ receptor cDNA was a gift of Dr. G. Buell (Ares-Serono, Geneva, Switzerland).

Cell Culture and Transfection Protocol. HEK-293, COS-7, and Chinese hamster embryonic fibroblast cells were maintained in exponential growth in Dulbecco's modified Eagle's medium supplemented with 10% heat-inactivated fetal bovine serum, 2 mM glutamine, 50 U/ml penicillin G, and 50 μg/ml streptomycin (Life Technologies, Inc., Rockville, MD). CHO-K1 cells were maintained in 50:50 Dulbecco's modified Eagle's medium/F12 medium (Cellgro, Herndon, VA) with the same supplements plus nonessential amino acid solution (Cellgro). All cells were incubated at 37°C in a humidified atmosphere with 5% CO_2. On reaching 70 to 80% confluence in 75cm^2 tissue culture flasks, the cells were trypsinized and then plated at a density of 3×10^5 cells/35-mm culture dish. The next day they were washed twice with serum free Opti-MEM (Life Technologies, Inc.) and transiently transfected with wild-type $P2X_1$ and/or $P2X_5$ receptor cDNAs. A mixture of 1 μg total cDNA and 6 μl Lipofectamine (Life Technologies, Inc.) in 1 ml of Opti-MEM was added to each plate for 5 h after which the bathing solution was replaced with the supplemented culture media. The cells were returned to the incubator and used for electrophysiological experiments 36 to 48 h later.

Electrophysiological Recordings. A suspension of transiently transfected cells were obtained by mechanical dissociation of the contents of a single 35-mm culture dish using a fire-polished Pasteur pipette. An aliquot of the cell suspension was transferred to a recording chamber mounted on the stage of an inverted microscope (Nikon Diaphot 200). The cells were continuously perfused with an extracellular bath solution containing: 150 mM NaCl, 1 mM $CaCl_2$, 1 mM $MgCl_2$, 10 mM glucose, 10 mM HEPES, pH 7.4 with NaOH, and whole-cell voltage clamp was performed using an AxoPatch 200A amplifier (Axon Instruments, Foster City, CA) with low resistance (1–2 MΩ) 7052 borosilicate glass electrodes (Garner Glass, Claremont, CA). The intracellular recording solution consisted of: 150 mM CsCl, 10 mM HEPES, 10 mM EGTA, and 10 mM tetraethylammonium-Cl, pH 7.4 with CsOH. Whole cell currents were measured at room temperature from single cells held at −40 mV. Drugs were applied by manually moving the electrode and attached cell into the line of flow of solutions exiting one of a group of inlet tubes feeding the recording chamber. Complete exchange of solution was obtained in less than 100 ms ($\tau \approx 24$ ms; T.M.E., unpublished observation). Unless otherwise stated, agonists were applied for about 2 s, separated by 1.5- to 2-min intervals; the exception was the $P2X_1$ receptor, where 3-min intervals were required to ensure recovery from desensitization. Antagonists were applied after a stable control ATP-evoked current amplitude was measured. Continuous application of antagonist began 1 min before the start of the test dose of agonist. Current-voltage relationships were determined for peak, plateau, and tail currents by measuring the response to 1 μM ATP in cells expressing $P2X_{1/5}$ and voltage-clamped at a range of potentials (−100 to +60 mV). Averaged data were fit with a third order polynomial to estimate the reversal potential. Liquid junction potentials were estimated to be 4.9 mV using Patcher's Power Tools (Dr. F. Mendez, Göttingen, Germany); no offset correction was used in the present study.

Drugs. Pyridoxal phosphate-6-azophenyl-2′,4′-disulfonic acid (PPADS) was purchased from Research Biochemicals, Inc. (Natick, MA), suramin was obtained from the Centers for Disease Control (Atlanta, GA), and 2′,3′-*O*-(2, 4, 6-trinitrophenyl) ATP (TNP-ATP) was purchased from Molecular Probes (Eugene, OR). All other drugs were purchased from Sigma (St. Louis, MO).

Data Analysis. Agonist concentration-response curves were generated by measuring peak currents evoked by a range of agonist concentrations. Currents from a single cell were normalized to those evoked by a test dose of 100 μM ATP in the same cell. The appropriate data from all cells were pooled and then fit using a Levenburg-Marquardt least-squares algorithm (IgorPro; Wavemetrics, Lake Oswego, OR) to the following equation:

$$I = I_{max}(1 - 1/(1 + ([\text{agonist}]/EC_{50})^{nH})) \quad (1)$$

where I_{max} is the maximum current at saturating concentrations of agonist, EC_{50} is the agonist concentration at which the response is half-maximal, and n_H is the Hill coefficient. Concentration-inhibition curves for antagonists were determined in a similar manner. The ability of a range of antagonist concentrations to inhibit peak currents evoked by 3 μM ATP was measured, the data were pooled, and the IC_{50} was determined from the best fit to

$$I = I_{max}(1/(1 + ([\text{antagonist}]/IC_{50})^{nH})) \quad (2)$$

where I_{max} is the normalized response to ATP in the absence of antagonist and IC_{50} is the antagonist concentration at which a 50% inhibition is apparent. Estimates of EC_{50} and IC_{50} are reported as mean ± S.D. as determined from the curve fits of the pooled data. All other data are mean ± S.E. Significance was determined using Student's t test.

Results

Homomeric $P2X_1$ and $P2X_5$ receptors differ in the size and shape of their ATP-gated currents and in their rank order of agonist and antagonist potencies. Cotransfection of HEK-293 cells with the cDNAs encoding the $P2X_1$ and $P2X_5$ isoforms results in expression of a heteromultimeric $P2X_{1/5}$ channel with a novel phenotype (Torres et al., 1998). We find that the phenotype of this heteromeric receptor incorporates features of both individual isoforms. Furthermore, the $P2X_{1/5}$ receptor has unique qualities that are not present in either homomeric $P2X_1$ or $P2X_5$ receptors.

The Effect of ATP. Figure 1A shows representative currents evoked by 30 μM ATP in HEK-293 cells expressing $P2X_1$, $P2X_5$, and $P2X_{1/5}$ receptors. ATP-gated current through the $P2X_1$ receptor differs from current through the $P2X_5$ receptor in two ways: current through $P2X_1$ is larger and is quicker to desensitize. By contrast, current through the heteromeric $P2X_{1/5}$ receptor is biphasic and has a fast inward current that quickly diminishes to a sustained plateau. That the biphasic current is not due to the simple superposition of $P2X_1$ and $P2X_5$ homo-oligomeric currents is supported by three findings. First, repeated and closely spaced applications of ATP produce near complete desensitization of homomeric $P2X_1$ receptors but causes little or no desensitization of peak current through the $P2X_{1/5}$ receptor (Torres et al., 1998). Second, the agonist profile of the sustained phase does not match that of the nondesensitizing $P2X_5$ receptor (see below). Third, modest concentrations of ATP elicits rebound tail currents in cells expressing the $P2X_{1/5}$ receptor, and this current is never recorded from cells expressing either $P2X_1$ or $P2X_5$ receptors alone. A typical response to an application of 30 μM ATP is shown in Fig. 1A (right). Current during the drug application was biphasic and had measurable peak and plateau currents. ATP-gated cur-

rent began to fade immediately on washout of agonist. This acute decline of membrane current reflects the rapid rate of solution exchange that we expect using the drug delivery system described in *Materials and Methods*. The initial decline was cut short, however, by the development of an additional phase of inward current that gradually reached a peak and then declined to the predrug-application holding current level. In most cells, the rebound tail current was as large or larger than the plateau current seen during the application of ATP. Tail currents were also measured in other mammalian expression systems including CHO-K1 (Fig. 1B), COS-7 (Fig. 1C), and Chinese hamster embryonic fibroblast (data not shown) cells, and are not unique to HEK-293 cells. The rebound tail current, however, is unique to the $P2X_{1/5}$ receptor, and we never recorded a similar current on removal of ATP or any other agonist from cells expressing any homomeric or other known heteromeric P2X receptor (data not shown). ATP-induced rebound currents have been demonstrated at high agonist concentrations in PC12 cells expressing P2X receptors as a result of acidification of the extracellular solution by addition of millimolar concentrations of ATP (Stoop and Quayle, 1998). The rebound tail current of $P2X_{1/5}$ receptors was not caused by acidification, because it was apparent at much lower concentrations (1–100 μM) of ATP that did not change the pH of the bathing solution and because tail current through the $P2X_{1/5}$ receptor is relatively insensitive to changes in pH (W.R.H. and T.M.E., unpublished observation).

Current-voltage curves were generated by measuring 1 μM ATP-gated currents of individual HEK-293 cells expressing the $P2X_{1/5}$ receptor. Individual currents evoked at a range of voltages (−100 to +60 mV) were measured at three different times during the ATP response, and the averaged currents at each potential were plotted against voltage (Fig. 2). The current-voltage relationships were not different for the peak, plateau, and rebound tail currents, suggesting that they all evolve from a common population of channels. Some inward rectification was seen at positive potentials, and all three currents had reversal potentials near 5 mV before correction for liquid junction potentials. Thus, $P2X_{1/5}$ receptors resemble other homomeric and heteromeric P2X receptors in being nonselective cation channels (Bean and Friel, 1993).

The Effects of Other Agonists. Raw currents elicited by applications of common purinoceptor agonists to cells expressing $P2X_{1/5}$ are shown in Fig. 3 where each row shows the response of a single cell to a different agonist applied at concentrations close to their EC_{20}, EC_{50}, and EC_{95} values. All agonists evoked monophasic, nondesensitizing currents when applied at the lowest effective concentrations. At the highest concentrations, the currents were biphasic and resembled those evoked by 100 μM ATP with two important differences. First, the ratio of size of the plateau current to the size of the rapidly developing peak current varied among agonists. The difference was greatest for ATP and 2-meSATP, which evoked large peak currents and relatively small plateau currents. By contrast, CTP evoked peak currents that were only slightly larger than the sustained plateaus.

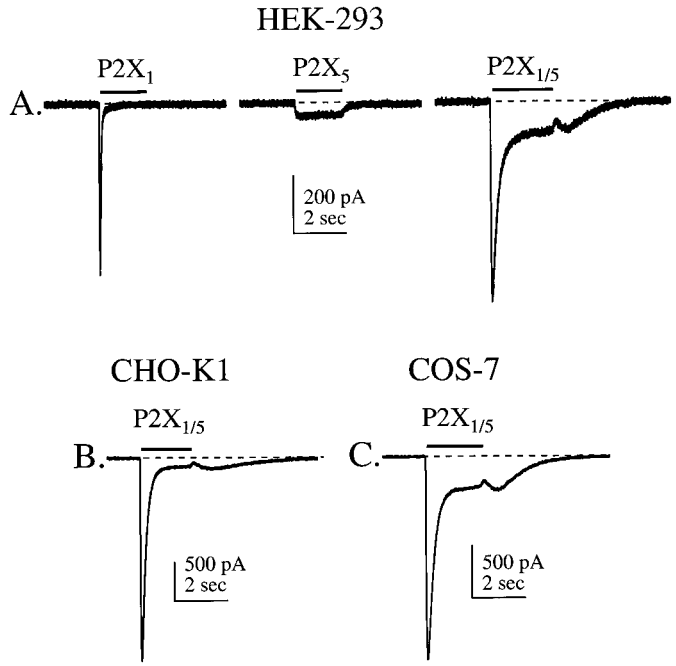

Fig. 1. Unique ATP-activated currents from cells coexpressing $P2X_1$ and/or $P2X_5$ receptor isoforms. Typical responses to 30 μM ATP are shown in cells voltage-clamped at −40 mV. A, HEK-293 cell transfected with cDNA encoding homomeric $P2X_1$ receptors showed the characteristic rapid desensitizing whole-cell current in response to ATP (left). By contrast, a different HEK-293 cell transfected with the cDNA encoding the $P2X_5$ receptor gave a small nondesensitizing current in response to ATP (middle). A third HEK-293 cell transfected with both cDNAs gave a biphasic current; note the pronounced tail of rebound inward current on washout of ATP (right). B and C, current phenotype observed from the hetero-oligomeric receptor in response to ATP was not unique to HEK-293 cells as similar currents were also observed in CHO-K1 (B) and COS-7 (C) cells coexpressing the two isoforms. Solid lines above all traces in this and the following figures indicate the approximate time of agonist application.

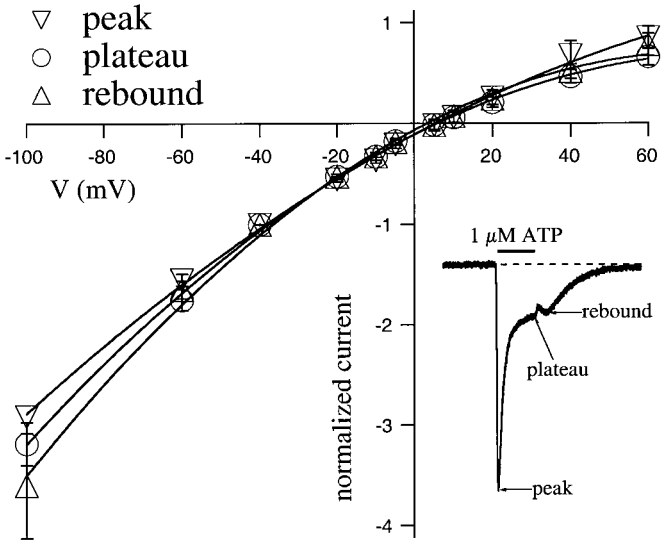

Fig. 2. Current-voltage relationships for $P2X_{1/5}$ receptor. Current-voltage relationships were examined by measuring the response to 1 μM ATP of individual HEK-293 cells expressing $P2X_{1/5}$ receptors and held at membrane potentials ranging from −100 to +60 mV. For each response the amplitude of the current was measured at three different phases (see inset). For all three phases, current amplitudes were normalized to those elicited at −40 mV and the averaged currents ± S.E.M. for all cells ($n \geq 3$) from a given potential were plotted against voltage. I-V curves for each measured phases were then generated by fitting the averaged data with a third order polynomial. Data shown is not corrected for liquid junction potentials estimated to be about 4.9 mV. Inset, typical current elicited by 1 μM ATP from a cell held at −40 mV. Peak, plateau, and rebound phases are labeled at points where current amplitudes were measured for generation of I-V curves.

Second, applications of some (ATP, 2-meSATP, ADP) but not all agonists were followed by generation of rebound tail currents. The size of the tail current was inversely related to the amplitude of the plateau current in that agonists (ATP, 2-meSATP) that generated small plateaus when applied at low concentrations also evoked large and long-lasting tail currents.

Agonist Sensitivity. Agonist potency was determined from the concentration-response curves of peak currents shown in Fig. 4; the results are summarized in Table 1. ATP and 2-meSATP were full and potent agonists with EC_{50} values of 0.7 ± 0.1 and 1.3 ± 0.3 μM, respectively. All other drugs evoked smaller peak currents and were less potent. The rank order of agonist potency measured from EC_{50} values for each drug was ATP ≥ 2-meSATP > adenosine 5′-*O*-(3-thiotriphosphate) (ATPγS) > α,β-methylene ATP (α,β-meATP) > ADP > CTP. α,β-methylene ADP (α,β-meADP); UTP; GTP; and AMP were poor agonists that evoked less than 5% of the maximal ATP current even when applied at the highest (100 μM) concentration. Most agonists (ATPγS; α,β-meATP; ADP; and CTP) evoked smaller peak currents than did ATP, suggesting that these drugs may be partial agonists. If so, then one would predict that concentration-response curves of these partial agonists would have lower slopes than those of the full agonist like ATP. However, we measured no significant differences in the Hill coefficients of these drugs and ATP, and other factors may explain the apparent change in efficacy. One possibility is that some agonists cause a rapid receptor desensitization that distorts the shape of their concentration-response curves. The most likely candidates are ATP and 2-meSATP, which apparently cause the greatest degree of rapid desensitization, and these agonists may be even more potent than our estimates reported here. A similar change in efficacy without a change in slope is also apparent in agonist concentration-response curves of the $P2X_1$ receptor (Valera et al., 1994).

Antagonist Sensitivity. Determination of the subunit composition of native P2X receptors is hampered by a lack of selective purinergic antagonists (Ralevic and Burnstock, 1998). However, a number of agents have been used to discriminate between the P2X and P2Y receptor families, and some newer drugs have shown limited selectivity for the different P2X isoforms. We tested three antagonists against ATP-evoked currents of the recombinant $P2X_{1/5}$ receptor. Two of these, suramin and PPADS, have been widely tested against purinergic responses of native tissues. The third, TNP-ATP, is a more selective antagonist of $P2X_1$ and $P2X_3$ receptors than of any other isoform (Virginio et al., 1998b). We measured the ability of increasing concentrations of each antagonist to block the currents evoked by applications of 3 μM ATP. Figure 5 shows raw data for each antagonist. The first trace in each family of currents represents the baseline ATP current before application of antagonist; as expected, ATP-generated inward current had the three distinct phases (rapid peak, sustained plateau, and rebound tail current) described above. The middle traces show the effect of different concentrations of antagonist, and the last trace shows the effect of the first postantagonist application of ATP. For suramin and TNP-ATP, a progressively larger block of ATP-gated current was apparent as the antagonist concentration increased (Fig. 5, top and middle). Peak current was affected first, although all three current components were antagonized. Near complete block of the ATP-induced current was attained with maximal concentrations of these antagonists (≥100 μM suramin and ≥30 μM TNP-ATP), and complete recovery of the response to ATP was seen within minutes of

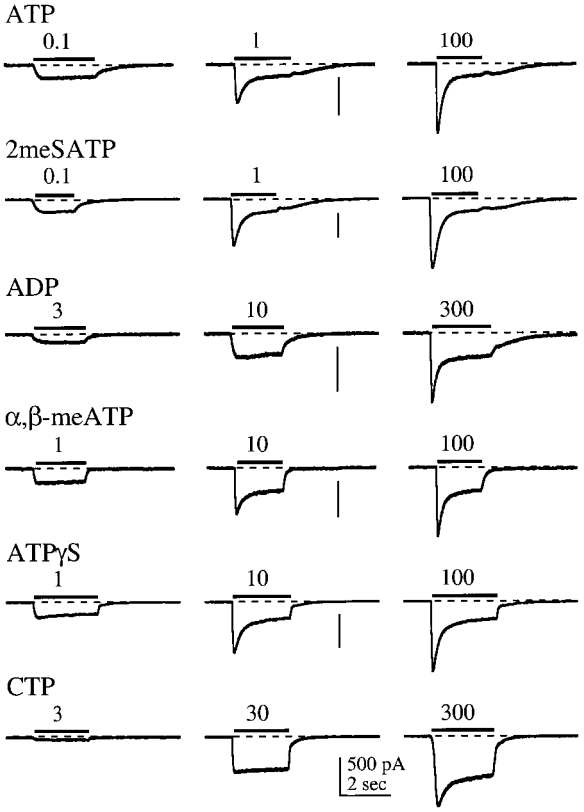

Fig. 3. Raw currents elicited by select P2X receptor agonists on $P2X_{1/5}$ receptors. Whole-cell currents recorded from HEK-293 cells held at −40 mV and expressing the hetero-oligomeric P2X receptor composed of $P2X_1$ and $P2X_5$ subunits. Each family of three traces was recorded from an individual cell and represents typical responses to three different concentrations of the agonist listed. Calibration: 500 pA, 2 s.

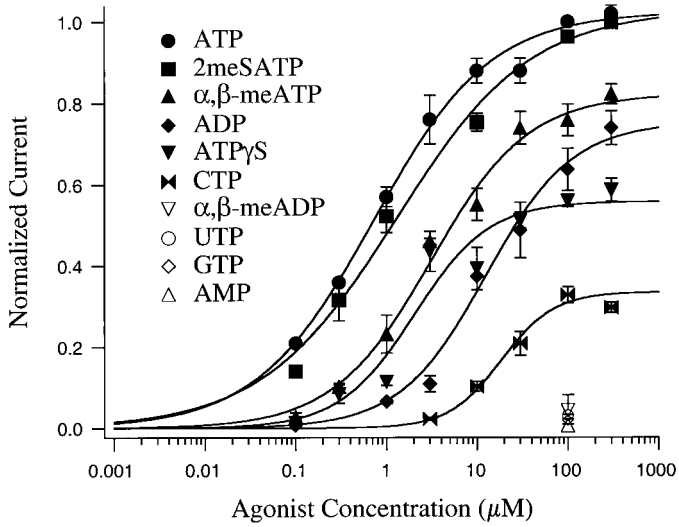

Fig. 4. Concentration-response curves for the actions of P2X receptor agonists on $P2X_{1/5}$ receptor. Peak currents evoked by a range of concentrations of each agonist were normalized to that obtained from 100 μM ATP. Only one other agonist was applied to each individual cell. Each point represents averaged normalized data ± S.E.M. Solid lines are the best fit to the pooled data as described in *Materials and Methods*.

their washout (data not shown). By contrast, the effect of PPADS was complex and varied with concentration. When applied in low concentrations (for example, see 0.1 μM PPADS, Fig. 5, bottom), PPADS had little effect on the peak ATP-gated current but markedly potentiated the plateau currents. These potentiations were irreversible (we tested up to 22 min after washout of PPADS). At higher concentrations, PPADS progressively inhibited all three current components until a near complete block of the ATP-response was achieved. The inhibition by PPADS reversed when the antagonist was removed. The molecular mechanism of the potentiation by PPADS is unknown. One possibility, however, is that some (ATP, 2-meSATP, ADP), but not all, agonists (for example, α,β-meATP) produce a pronounced receptor desensitization that can be modulated by PPADS; this hypothesis is supported by the data in Fig. 6. In this experiment, the ability of two concentrations of PPADS to alter currents evoked by α,β-meATP and ATP were measured in a single HEK-293 cell expressing $P2X_{1/5}$ receptors. As expected, α,β-meATP evoked large peak and plateau currents, whereas the plateau current evoked by ATP was smaller. If the smaller plateau current measured in ATP reflects an agonist-specific receptor desensitization sensitive to PPADS, then a low concentration of this antagonist would be expected to alter the shape of the ATP-gated current so that it more closely resembles that caused by α,β-meATP. This is exactly what happens. The shapes of the currents evoked by both ATP and α,β-meATP were similar when applied in the presence of 0.1 μM PPADS, a concentration of antagonist that caused only a small effect on the peak current amplitudes. The data also suggest that a separate population of lower-affinity PPADS binding sites is responsible for inhibition of both α,β-meATP and ATP currents, as higher concentrations of PPADS inhibited peak currents caused by either antagonist to an equal degree (see Fig. 6).

Antagonist IC_{50} values were determined from the inhibition of peak currents. Concentration-response curves are shown in Fig. 7, and the data are summarized in Table 2. TNP-ATP is a potent antagonist of homomeric $P2X_1$ receptors with an IC_{50} of 1 to 3 nM when tested against ATP

TABLE 1

Summary of agonist properties

EC_{50} was determined from a three-parameter (EC_{50}, I_{max}, n_H) curve fit to pooled data as described in *Materials and Methods*; estimates are expressed as mean ± S.D. EPMR, equipotent molar ratio and equals (EC_{50}, test agonist)/(EC_{50}, ATP). *N*, number of cells contributing to the pooled data for each agonist.

Agonist	EC_{50}	I_{max}	n_H	EPMR	*N*
	μM				
ATP	0.7 ± 0.1	1.0	0.7	1	9
2meSATP	1.3 ± 0.3	1.0	1.3	1.9	9
ATPγS	2.0 ± 0.5	0.6	1.1	2.9	6
α,β-meATP	3.1 ± 0.6	0.6	0.8	4.4	6
ADP	13 ± 3.3	0.8	0.9	18.6	10
CTP	18.6 ± 3.7	0.3	1.5	26.5	10

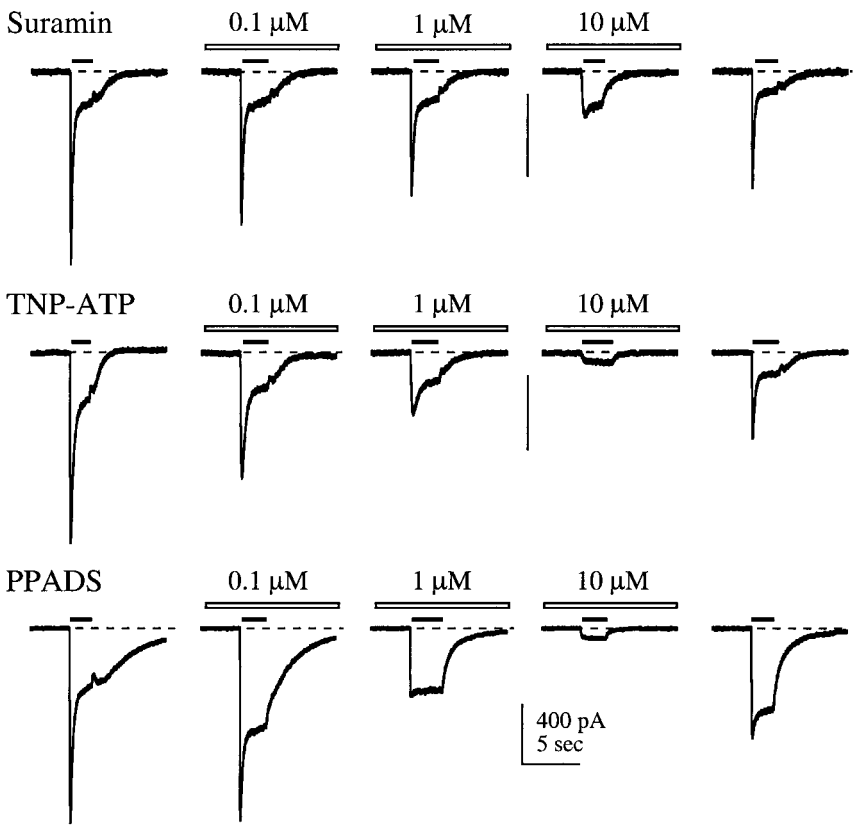

Fig. 5. Effects of P2X antagonists on raw current elicited by ATP through $P2X_{1/5}$ receptors. Whole-cell currents recorded from HEK-293 cells expressing $P2X_{1/5}$ receptors. Each family of five traces was recorded from an individual cell voltage-clamped at −40 mV and demonstrates the inhibitory effects of increasing concentrations of the listed antagonist on responses to 3 μM ATP. The first and last trace in each family represents the control ATP response and first ATP response after washout of the antagonist, respectively. Open horizontal bars denote currents recorded in the presence of the given antagonist. All antagonists were applied 1 min before, as well as during, ATP application. Calibration: 400 pA, 5 s.

applied at concentrations close to its EC_{50} (Virginio et al., 1998b; W.R.H. and T.M.E., unpublished observation). We found that this drug was far less potent in inhibiting peak current through $P2X_{1/5}$ receptor, where it had an IC_{50} of 0.36 ± 0.13 μM. Homomeric $P2X_1$ and $P2X_5$ receptors do not differ dramatically in their sensitivity to PPADS and suramin. Not surprising then is the finding that the sensitivity of the heteromeric $P2X_{1/5}$ receptor to PPADS (IC_{50} equals 0.63 ± 0.05 μM) and suramin (IC_{50} equals 1.6 ± 0.7 μM) resembled those of the homomeric receptors.

The Effect of Extracellular Calcium. ATP-gated current through the $P2X_1$ receptor is relatively insensitive to changes in extracellular $[Ca^{2+}]$ (Evans et al., 1996; Virginio et al., 1998a; Fig. 8, top). The sensitivities of $P2X_5$ and $P2X_{1/5}$ receptors are unknown. We measured the ability of increasing concentrations of $[Ca^{2+}]_o$ to alter ATP-gated current in cells expressing either $P2X_1$, $P2X_5$, or $P2X_{1/5}$ receptors. Current evoked by 15 μM ATP through $P2X_5$ receptors was strongly inhibited by raising $[Ca^{2+}]_o$ with an apparent IC_{50} of 6.7 ± 1.9 mM (Fig. 8, middle). By contrast, peak currents through $P2X_{1/5}$ receptors were unaffected by changes in $[Ca^{2+}]_o$ (Fig. 8, bottom). However, increasing $[Ca^{2+}]_o$ potentiated plateau currents evoked by 3 μM ATP, perhaps by the same mechanism that underlies the potentiation of this phase of current by PPADS. No enhancement was seen when Ba^{2+} was substituted for extracellular Ca^{2+}, and chelating $[Ca^{2+}]_i$ by addition of 20 mM BAPTA to the pipette solution had no effect on the magnitude of the rebound current (data not shown). These results suggest that the effect of Ca^{2+} does not involve an intracellular pathway, but may involve a Ca^{2+}-specific effect on a part of the channel protein accessible from the bath solution. A summary of the effects of $[Ca^{2+}]_o$ on currents through $P2X_1$, $P2X_5$, and $P2X_{1/5}$ is presented in Fig. 9.

Discussion

The unique properties of some native ATP-induced currents might result from formation of novel P2X receptors by hetero-oligomeric assembly of different receptor isoforms. Evidence is now mounting to support this hypothesis. Multiple P2X receptor isoforms are expressed in many of the same tissues (Ralevic and Burnstock, 1998). Furthermore, most P2X receptor isoforms (the exception is $P2X_7$) can form hetero-oligomeric assemblies (Torres et al., 1999). Finally, novel receptors formed by heteropolymerization of $P2X_2$ and $P2X_3$ (Lewis et al., 1995), $P2X_1$ and $P2X_5$ (Torres et al., 1998), and $P2X_4$ and $P2X_6$ (Le et al., 1998) have been shown to functionally assemble in heterologous cell systems. A more complete survey of ATP-gated currents of native tissues therefore critically depends on a complete functional characterization of the possible combinations of heteromultimeric assemblies. We present here an extensive characterization of the novel $P2X_{1/5}$ receptor expressed in HEK-293 cells. Results from in situ hybridization, PCR/cloning analysis, and immunocytochemistry experiments have implicated the coexistence of $P2X_1$ and $P2X_5$ receptors in heart (Bogdanov et al., 1998) and spinal cord tissue (Collo et al., 1996), and our results provide a basis for subsequent investigation of the effects of extracellular ATP in those tissues.

The pharmacological profile of the $P2X_{1/5}$ receptor is different from that of either the $P2X_1$ and $P2X_5$ homo-oligomeric receptors and borrows unique traits from each isoform. The agonist potency ranked by EC_{50} was ATP ≥ 2-meSATP > ATPγS > α,β-meATP > ADP > CTP. Thus, like the $P2X_5$ receptor, ATP is slightly more potent than 2 meSATP at the $P2X_{1/5}$ receptors. However, unlike the $P2X_5$ receptor (but like $P2X_1$ receptors), the $P2X_{1/5}$ receptor is appreciably sensitive to α,β-meATP. Indeed, the ability of α,β-meATP to activate biphasic currents with large plateaus is probably the most distinguishing characteristic of the $P2X_{1/5}$ phenotype. $P2X_{1/5}$ receptors also show large sustained currents in response to the pyrimidine nucleotide, CTP, a property not shared by the $P2X_5$ receptor (Garcia-Guzman et al., 1996). $P2X_{1/5}$ receptors are as sensitive to the antagonists suramin and PPADS as are $P2X_1$ and $P2X_5$ receptors, but they are markedly less sensitive to TNP-ATP than the $P2X_1$ receptor. Furthermore, the novel heteromultimeric receptor resembles the $P2X_1$ receptor in the inability of a rise in extracellular calcium to block peak ATP-gated current.

The dual effects (e.g., potentiation and block) of PPADS on the shape of ATP-gated currents are unique to $P2X_{1/5}$ receptors. One explanation is that cotransfection of HEK-293 cells with cDNAs encoding the $P2X_1$ and $P2X_5$ isoforms leads to at least two separate populations of heteromultimeric receptors that differ in their response to PPADS. If so, then the agonist and antagonist profiles of these two populations must be very similar because all of the concentration-response curves were well fit using models that assume either a homogenous re-

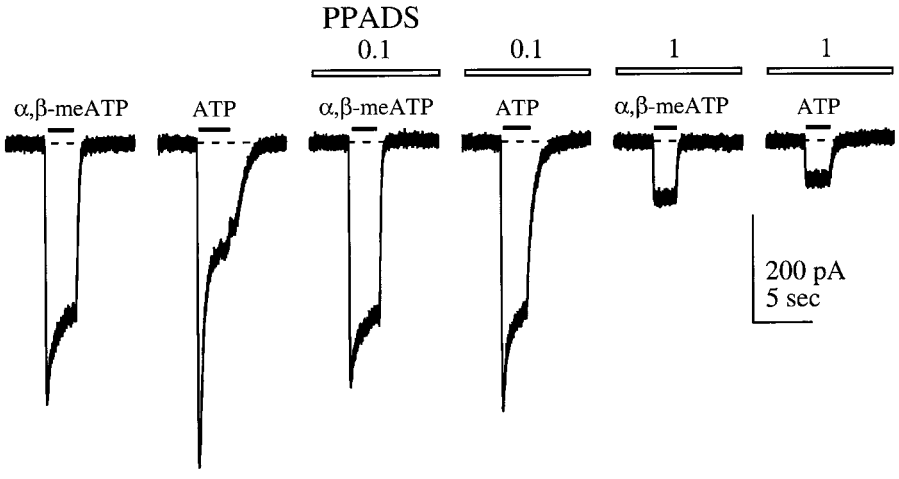

Fig. 6. Effects of PPADS on raw $P2X_{1/5}$ currents elicited by ATP and α,β-meATP. Whole-cell currents recorded from HEK-293 cells expressing $P2X_{1/5}$ receptors. All currents were recorded from a single cell voltage clamped at −40 mV and represent the effects of two different doses of PPADS on both 10 μM α,β-meATP- and 1 μM ATP-evoked currents. Open horizontal bars denote currents recorded in the presence of PPADS. Calibration: 200 pA, 5 s.

ceptor population or multiple populations with identical parameters. Another possibility is that PPADS (and $[Ca^{2+}]_o$) affect receptor desensitization in an agonist-specific manner. Thus, full agonists like ATP and 2-meSATP cause a rapid decline in current as the receptor desensitizes, whereas partial agonists like α,β-meATP cause less desensitization and have larger plateaus. ADP is an exception to this rule; it is not a full agonist but it does have a pronounced rebound tail current when applied in high (300 μM) concentrations. This prominent tail current may result from contamination of ADP with ATP. Regardless, if the rate of desensitization is lengthened by application by PPADS, then we would expect this drug to have its greatest effect on those responses that show the greatest desensitization; this is exactly the case. Application of 0.1 μM PPADS greatly increases the size of the plateau current evoked by ATP, changing the shape of the response so that it closely resembles the current evoked by α,β-meATP. This model assumes that there are at least two populations of PPADS binding sites: a high-affinity site that results in change in receptor desensitization and a lower-affinity site that results in noncompetitive inhibition of current. This is because higher concentrations of PPADS inhibited all current components equally well. The presence of multiple populations of PPADS binding sites is also supported by the Hill slope of this antagonist's concentration-response curves (Fig. 7 and Table 2). Furthermore, raising $[Ca^{2+}]_o$ would have an effect like PPADS if the rate of desensitization can also be modulated by Ca^{2+}. Indeed, the time course of desensitization of homomeric $P2X_3$ receptors is modulated by changes in $[Ca^{2+}]_o$ (Cook and McCleskey,

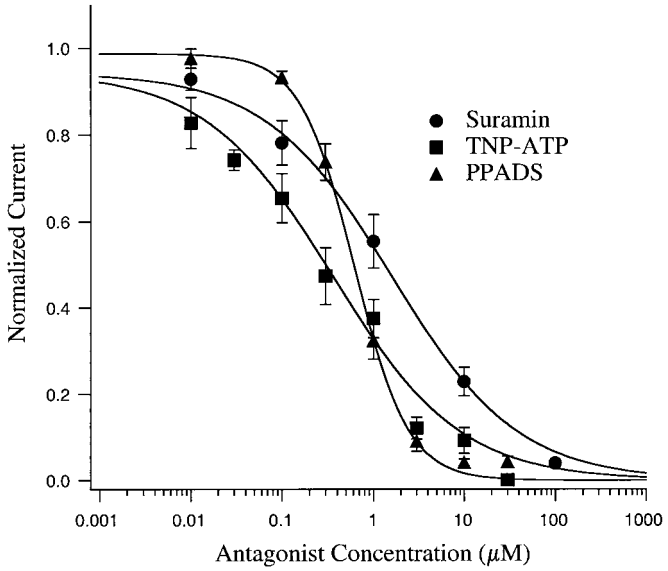

Fig. 7. Concentration-inhibition curves for P2X receptor antagonists on $P2X_{1/5}$ receptors. The curves were generated by measuring peak currents evoked by 3 μM ATP in the presence of varying concentrations of each antagonist in single cells. Only one antagonist was applied to each individual cell. The currents were normalized to those evoked by 3 μM ATP in the same cell. Each point represents averaged normalized data ± S.E.M. Solid lines are the best fit to the pooled data as described in *Materials and Methods*.

TABLE 2

Summary of antagonist properties

IC_{50} was determined from a three-parameter (IC_{50}, I_{max}, n_H) curve fit to pooled data as described in *Materials and Methods*; estimates are expressed as mean ± S.D. *N*, number of cells contributing to the pooled data for each agonist.

Antagonist	IC_{50} (μM)	n_H	*N*
PPADS	0.63 ± 0.05	1.5	8
Suramin	1.6 ± 0.7	0.6	8
TNP-ATP	0.36 ± 0.13	0.6	8

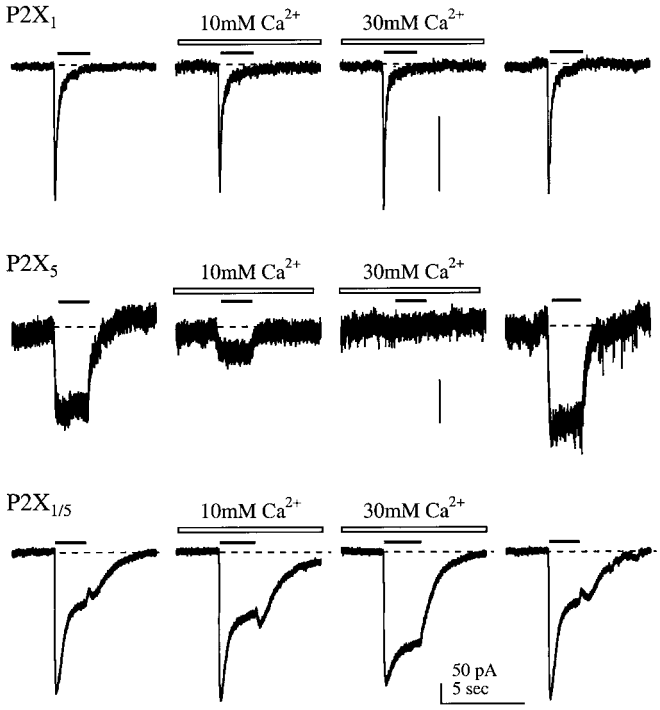

Fig. 8. Sensitivity of $P2X_{1/5}$ receptors to changes in extracellular calcium concentration. The effects of increasing concentrations of extracellular calcium on ATP-activated currents recorded from cells expressing $P2X_1$ and/or $P2X_5$ receptors were investigated. Typical responses are shown. Changing the extracellular calcium concentration from 1 to 10 or 30 μM had no effect on the amplitude of the current elicited by 3 μM ATP in cells expressing only $P2X_1$ receptors (top). However, a change in the extracellular calcium concentration from 1 to 10 μM greatly inhibited currents evoked by 15 μM ATP in a cell expressing $P2X_5$ receptors alone; further increasing the extracellular calcium to 30 mM completely and reversibly abolished the ATP-activated current (middle). In a cell expressing the hetero-oligomeric $P2X_{1/5}$ receptor, increasing calcium concentrations had no effect on peak current amplitude elicited by 3 μM ATP, although a reversible dose-dependent increase in the plateau phase was observed (bottom). Current through $P2X_1$ receptor was filtered at 300 Hz; other traces were filtered at 5 KHz.

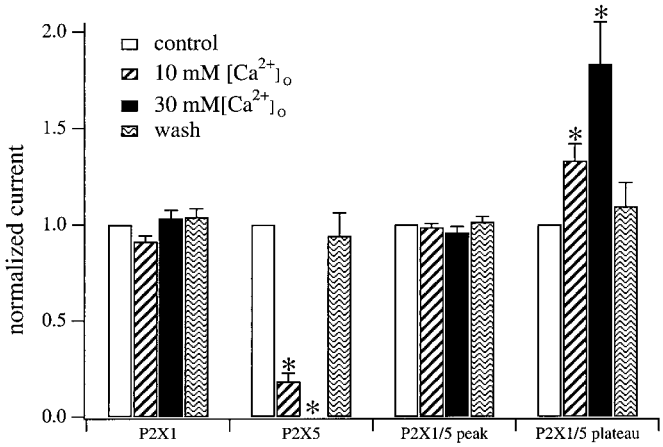

Fig. 9. Pooled data from experiments described in Fig. 8. Data are mean ± S.E. Data significantly different ($p < .01$) from control currents recorded in 1 mM $[Ca^{2+}]_o$ are marked with asterisks.

1997), and a similar mechanism may be present in $P2X_{1/5}$ receptors. It will be interesting to see if site-directed mutagenesis identifies common or different sites underlying the similar effects of $Ca^{2+}{}_o$ and PPADS on desensitization.

The agonist-dependent change in receptor desensitization may also explain the genesis of the rebound tail current. Full agonists that have pronounced desensitization also have the largest rebound tail currents. If recovery from desensitization can only occur from the open state, then a channel would need to cycle from the desensitized, to the open, to the closed state on removing agonist; rebound current could occur if the cycle is slow. Of course, other explanations are also possible. For example, the tail current may result from relief of open channel block perhaps by ATP itself. However, the size of the tail current is an approximately linear function of voltage, and this lack of voltage dependence argues against such a mechanism. Additional experiments are needed to more fully understand the mechanisms that underlie generation of this current component.

Several native fast-acting ATP responses have been recorded although the subtype of P2X receptor mediating these responses is still unknown. In pyramidal neurons of the CA1 area of the rat hippocampus, both excitatory postsynaptic currents from hippocampal slices and ATP-activated whole cell currents sensitive to PPADS have been identified (Pankratov et al., 1998). ATP and similar analogs also elicit fast rising inward currents attributable to activation of P2X receptors in trigeminal mesencephalic nucleus neurons of the rat (Khakh et al., 1997). Finally, P2X purinoceptors were shown to mediate excitatory effects in rat locus ceruleus neurons (Sansum et al., 1998). The specific P2X receptor isoform(s) which mediate these different purinergic responses have yet to be conclusively identified, and it is possible that a hetero-oligomeric P2X receptor might account for the different responses. mRNAs encoding the $P2X_1$ and $P2X_5$ isoforms are both found in large neurons of the ventral horn of the rat spinal cord (Collo et al., 1996), raising the possibility that native heteromeric $P2X_{1/5}$ receptors may exist. Here, we have presented data further characterizing the pharmacological profile of the novel recombinant $P2X_{1/5}$ ionotropic receptor. These data should provide the foundation for functional identification of purinergic responses of native systems.

Acknowledgments

We thank Laura Hobart for help with tissue culture, transfections, reading the manuscript, and work on Saturdays; Shelly Strickfaden for technical assistance; and Baljit Singh Khakh for his constructive criticism of the experiments and manuscript.

References

Barnard EA (1992) Receptor classes and the transmitter-gated ion channels. *Trends Biochem Sci* **17:**368–374.

Bean BP and Friel DD (1993) ATP-activated channels in excitable cells, in *Ion Channels* (Narahashi T ed) pp 169–203, Plenum Press, New York.

Betz H (1990) Ligand-gated ion channels in the brain: The amino acid receptor superfamily. *Neuron* **5:**383–392.

Bogdanov Y, Rubino A and Burnstock G (1998) Characterisation of subtypes of the P2X and P2Y families of ATP receptors in the foetal human heart. *Life Sci* **62:**697–703.

Brake AJ and Julius D (1996) Signaling by extracellular nucleotides. *Annu Rev Cell Dev Biol* **12:**519–541.

Claudio T (1992) Stable expression of heterologous multisubunit protein complexes established by calcium phosphate- or lipid-mediated cotransfection. *Methods Enzymol* **207:**391–408.

Collo G, North RA, Kawashima E, Merlo-Pich E, Neidhart S, Surprenant A and Buell G (1996) Cloning of P2X5 and P2X6 receptors and the distribution and properties of an extended family of ATP-gated ion channels. *J Neurosci* **16:**2495–2507.

Cook SP and McCleskey EW (1997) Desensitization, recovery and Ca^{2+}-dependent modulation of ATP-gated P2X receptors in nociceptors. *Neuropharmacology* **36:** 1303–1308.

Evans RJ, Lewis C, Virginio C, Lundstrom K, Buell G, Surprenant A and North RA (1996) Ionic permeability of, and divalent cation effects on, two ATP-gated cation channels (P2X receptors) expressed in mammalian cells. *J Physiol (Lond)* **497:** 413–422.

Garcia-Guzman M, Soto F, Laube B and Stuhmer W (1996) Molecular cloning and functional expression of a novel rat heart P2X purinoceptor. *FEBS Lett* **388:**123–127.

Khakh BS, Humphrey PP and Henderson G (1997) ATP-gated cation channels (P2X purinoceptors) in trigeminal mesencephalic nucleus neurons of the rat. *J Physiol (Lond)* **498:**709–715.

Khakh BS, Surprenant A and Humphrey PP (1995) A study on P2X purinoceptors mediating the electrophysiological and contractile effects of purine nucleotides in rat vas deferens. *Br J Pharmacol* **115:**177–185.

Le KT, Babinski K and Seguela P (1998) Central P2X4 and P2X6 channel subunits coassemble into a novel heteromeric ATP receptor. *J Neurosci* **18:**7152–7159.

Lewis C, Neidhart S, Holy C, North RA, Buell G and Surprenant A (1995) Coexpression of $P2X_2$ and $P2X_3$ receptors subunits can account for ATP-gated currents in sensory neurons. *Nature (Lond)* **377:**432–435.

Pankratov Y, Castro E, Miras-Portugal MT and Krishtal O (1998) A purinergic component of the excitatory postsynaptic current mediated by P2X receptors in the CA1 neurons of the rat hippocampus. *Eur J Neurosci* **10:**3898–3902.

Ralevic V and Burnstock G (1998) Receptors for purines and pyrimidines. *Pharmacol Rev* **50:**413–492.

Sansum AJ, Chessell IP, Hicks GA, Trezise DJ and Humphrey PP (1998) Evidence that P2X purinoceptors mediate the excitatory effects of α,β-methylene-ADP in rat locus coeruleus neurones. *Neuropharmacology* **37:**875–885.

Stoop R and Quayle JM (1998) Fading and rebound of P2X2 currents at millimolar ATP concentrations caused by low pH. *Br J Pharmacol* **125:**235–237.

Surprenant A, Buell G and North RA (1995) P_{2X} receptors bring new structure to ligand-gated ion channels. *Trends Neurosci* **18:**224–229.

Torres G, Haines W, Egan T and Voigt M (1998) Co-expression of $P2X_1$ and $P2X_5$ receptor subunits reveals a novel ATP-gated ion channel. *Mol Pharmacol* **54:**989–993.

Torres GE, Egan TM and Voigt MM (1999) Hetero-oligomeric assembly of P2X receptor subunits. Specificities exist with regard to possible partners. *J Biol Chem* **274:**6653–6659.

Valera S, Hussy N, Evans RJ, Adami N, North RA, Suprenant A and Buell G (1994) A new class of ligand-gated ion channel defined by P_{2x} receptor for extracellular ATP. *Nature (Lond)* **371:**516–519.

Virginio C, North RA and Surprenant A (1998a) Calcium permeability and block at homomeric and heteromeric P2X2 and P2X3 receptors, and P2X receptors in rat nodose neurones. *J Physiol (Lond)* **510:**27–35.

Virginio C, Robertson G, Surprenant A and North RA (1998b) Trinitrophenyl-substituted nucleotides are potent antagonists selective for P2X1, P2X3, and heteromeric P2X2/3 receptors. *Mol Pharmacol* **53:**969–973.

Vulchanova L, Riedl MS, Shuster SJ, Buell G, Surprenant A, North RA and Elde R (1997) Immunohistochemical study of the P2X2 and P2X3 receptor subunits in rat and monkey sensory neurons and their central terminals. *Neuropharmacology* **36:**1229–1242.

Send reprint requests to: Dr. William R. Haines, Department of Pharmacological and Physiological Science, St. Louis University School of Medicine, 1402 S. Grand Blvd., St. Louis, MO 63104. E-mail: haineswr@slu.edu